EXTROVERT

ADVANCED CONCEPT EXPLORATION

ADL P-2013043001

Josh Sandler, Mark Lieberbaum

Georgia Institute of Technology
School of Aerospace Engineering

FAHLLS

Frequent Access Heavy Lift Launch System

May 2, 2013

Publishing Information

We gratefully acknowledges support under the NASA Innovation in Aerospace Instruction Initiative, NASA Grant No. NNX09AF67G, to develop the techniques that allowed such work to be done in core courses, and the resources used to publish this. Tony Springer is the Technical Monitor.

Disclaimer

Runway-Based Space Launch System Aerodynamics

Josh Sandler and Mark Lieberbaum

AE3021A

April 30, 2013

Contents

1 Introduction **3**

2 Background Research **5**
2.1 Heavy Lift Vehicles 5
2.2 Hypersonic Airbreathing Vehicles 5
2.3 Horizontal Takeoff Spacecraft 7
2.4 Overall Concept 9

3 Vehicle Sizing **11**

4 Aerodynamics and Propulsion **17**
4.1 Stage 1 17
4.1.1 Skin Friction Drag 17
4.2 Stage 2 and Stage 3 18
4.2.1 Subsonic 20
4.2.2 Supersonic 21
4.2.3 Hypersonic 21
4.2.4 Stage 2 Simulation Results 22
4.2.5 Stage 3 Trajectory Simulation 26
4.2.6 Stage 3 Trajectory Simulation Results 28

5 Conclusion **33**

List of Figures

2.1 X-43 Rendering. (Source [4]) 6
2.2 X-51 Rendering. (Source [7]) 6
2.3 HTV-3X Rendering. (Source [9]) 7
2.4 X-30 Rendering. (Source [10]) 7
2.5 HOTOL Rendering. (Source [15]) 8
2.6 Lynx Rendering. (Source [13]) 9

4.1 Stage 2 Mach number vs. altitude 19
4.2 Stage 2 Mass vs. altitude 20
4.3 Stage 2 Total drag vs. altitude 23
4.4 Stage 2 Induced/pressure drag vs. altitude 24
4.5 Stage 2 skin friction drag vs. altitude 25
4.6 Stage 2 angle of attack vs. altitude 26
4.7 Stage 3 Mach number vs. altitude 27
4.8 Stage 3 mass vs. altitude 28
4.9 Stage 3 Total drag vs. altitude 29
4.10 Stage 3 Induced/pressure drag vs. altitude 30
4.11 Stage 3 skin friction drag vs. altitude 31
4.12 Stage 3 angle of attack vs. altitude 32

List of Tables

2.1 Heavy Lift Aircraft 5

3.1 3rd Stage, 10% Payload Fraction 12
3.2 2nd Stage, 10% Payload Fraction 12
3.3 1st Stage, 10% Payload Fraction 13
3.4 3rd Stage, Optimal 13
3.5 2nd Stage, Optimal 14
3.6 1st Stage, Optimal 14

Chapter 1

Introduction

Over 40 years, Space Solar Power must deliver 4 billion kilograms to Earth orbit in order to eliminate the necessity to use fossil fuels on Earth. This is equivalent to 1000 payloads per year, each weighing 100,000 kg. It is desired to launch these payloads at the rate of approximately 3 per day in to low Earth orbit using a completely reusable, runway-based heavy lift launch system. The proposed system, FAHLLS (Frequent Access Heavy Lift Launch System), is a three-stage launch system which delivers 100,000 kg to low Earth orbit. Each stage is completely reusable. The first stage is a heavy lift aircraft, which carries the second and third stages to an altitude of 50,000 feet and Mach 0.8, operating on turbofan engines. The second stage is a delta-wing waverider, which carries the third stage to 200,000 feet and Mach 15, using a combination turbojet/RAMJet/SCRAMJet experimental propulsion system. The third stage carries the payload the remainder of the way to low Earth orbit, operating on traditional liquid rocket engines. This paper describes the design, sizing, and aerodynamic calculations for each of the stages of FAHLLS.

Chapter 2

Background Research

2.1 Heavy Lift Vehicles

A summary of current and proposed heavy lift aircraft can be seen below in Table 2.1.

Aircraft	**Takeoff Weight (kg)**	**Payload (kg)**	**Wing Span (m)**
Lockheed C-5 Galaxy	381,000	122,470	67.89
Boeing C-17 Globemaster III	265,350	77,519	51.75
Antonov An-124	405,000	150,000	73.3
Antonov An-225	1,410,958	-	88.4
Boeing 747 Dreamlifter	364,235	-	64.4
Beriev Be-2500	2,500,000	1,000,000	156
Scaled Composites Stratolaunch	1,200,000	-	117
Airbus A380F	590,000	149,800	79.75
Aerospacelines Super Guppy	77,110	24,720	47.625

Table 2.1: Heavy Lift Aircraft

2.2 Hypersonic Airbreathing Vehicles

1. The X-43 is a NASA unmanned experimental hypersonic aircraft that flew most recently on November 14, 2004. The X-43 is launched from a carrier aircraft and uses a booster rocket to accelerate it before its scramjet is turned on (once it reaches Mach 4.5). In 2004 the X-43 set a speed record of 10,617 km/hr (Mach 9.65) at 33,528 m. The scramjet operated for 10 seconds and burnt approximately 1 kg of Hydrogen fuel. The vehicle is approximately 3.7 m long and is a lifting body. It used water-cooling inside the surfaces to prevent the vehicle from melting, but was only a single use vehicle.

Figure 2.1: X-43 Rendering. (Source [4])

2. The X-51 WaveRider is a Boeing developed experimental hypersonic aircraft which first flew on May 26, 2010 and is a successor to the X-43. Similarly to the X-43, the X-53 is carried to an altitude of 15.2 km and then accelerated to Mach 4.5 by a solid booster rocket before its scramjet engine (Pratt and Whitney Rocketdyne SJY61) is activated. The X-53 carries 120 kg of JP-7 for the scramjet and can reach Mach 6. The X-53s longest flight had a scramjet burn time of 140 seconds at 21,000 m and reached Mach 5. Longer and faster flights were planned, but suffered failures. The X-51 is 7.62 m long and is a lifting body.

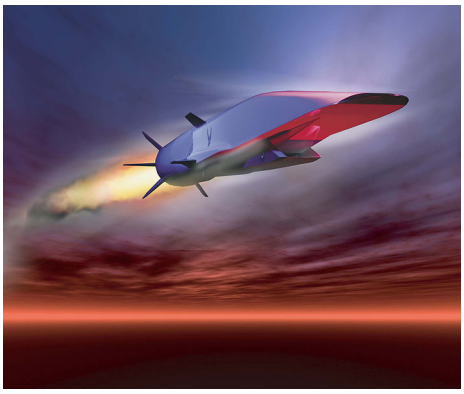

Figure 2.2: X-51 Rendering. (Source [7])

3. The Falcon Project was a DARPA and USAF joint project that included the development of a hypersonic vehicle called the HTV-3X Blackswift, however Blackswift was cancelled in 2008. The vehicle was intended to take off from a runway and fly at Mach 6. It would've used a combination of a turbine engine to accelerate to Mach 3 and a ramjet above Mach 3. Though the HTV-3X never flew, two HTV-2s were tested. The vehicles were launched from Minotaur IV rockets and were intended to reach Mach 20, but both tests lost contact with the ground before their flights were completed.

Figure 2.3: HTV-3X Rendering. (Source [9])

2.3 Horizontal Takeoff Spacecraft

1. The X-30 was intended to be a passenger space plane, taking off and landing horizontally, that was developed by Rockwell International in the 1980's and early 1990's. While the ultimate goal was for it to be able to carry passengers into orbit, the initial prototype was to carry two pilots. This was to be an air breathing single-state-to-orbit space plane. Most of the lift was to be generated by the fuselage at an angle of attack. The wings were very small, and existed simply for control of the space plane. Due to hot operating temperatures, special alloys had to be developed. Approximately 3000 degrees F was expected in some places on the space plane. The development continued well into the design phase; wind tunnel tests were performed, and special alloys were developed. The spaceplane as designed was 160 feet long, with a 74 foot wingspan. It had a takeoff weight of 300,000 pounds, and the propulsion device was a scramjet engine that ran on air and liquid hydrogen. Unfortunately, in 1993, the project was cancelled, due to budgetary and technical issues.

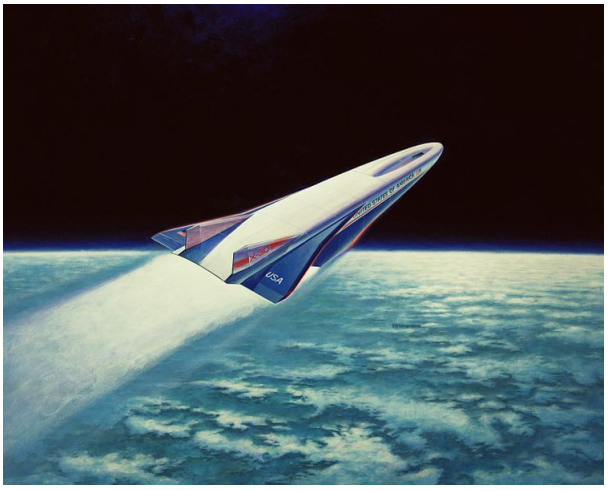

Figure 2.4: X-30 Rendering. (Source [10])

2. HOTOL (Horizontal Take-Off and Landing) was a conceptual vehicle that was created by the British. It was intended as a horizontal take off and landing, single stage to orbit, air breathing vehicle. Unfortunately, this was only a conceptual vehicle, and never was made a reality. It was to have dimensions similar to a medium-sized transport airliner. The plan was for HOTOL to take off from a runway while riding on the back of a large booster rocket, which got HOTOL to about 30 km in altitude, and to roughly Mach 6. At this point, the propulsion would switch from jet propulsion to rocket propulsion, and HOTOL would then enter orbit. It could place 7-8 metric tons in a 300 km circular orbit before reentering and gliding back to a runway, to land like a conventional aircraft. The project died around 1988 as it was nearing the end of its design cycle. It went downhill due to aerodynamic problems and fear of continuing to fund it.

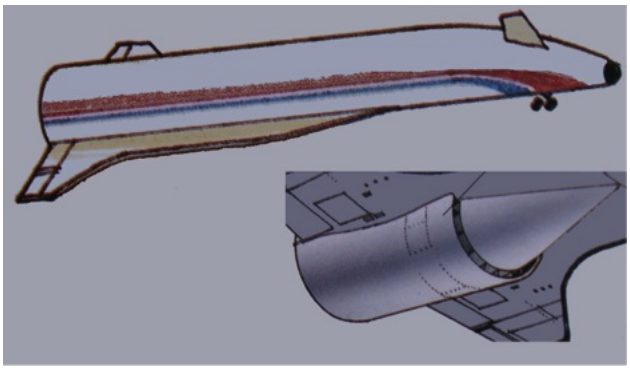

Figure 2.5: HOTOL Rendering. (Source [15])

3. The Lynx suborbital space plane is a space plane currently being designed by XCOR Aerospace in Mojave, California. This space plane takes off and lands horizontally on a runway. The Lynx space plane uses four LOX-Kerosene engines, each producing 2900 pounds of thrust. The Lynx is only capable of subortal spaceflight, and is designed to take a pilot and a passenger up to the edge of space before gliding back down to earth to land on a runway. There are two versions of the Lynx. The Mark I is a prototype, with a maximum altitude of 62 km, while the Mark II is capable of altitudes equal to or greater than 100 km. The Lynx is also capable of taking a 120 kg payload up to these altitudes. The Lynx is designed to be able to make trips to space up to four times per day, indicating great reusability and robustness. The Lynx space plane is still under development, and is expected to have its first flight tests in the very near future.

Figure 2.6: Lynx Rendering. (Source [13])

2.4 Overall Concept

As seen in Table 2.1, many aircraft capable of lifting large payloads have been developed. Our initial concept is to use a minimalistic large aircraft (similar to the Stratolaunch carrier aircraft) as the first stage. This aircraft will takeoff and land from a runway and takeoff may be assisted by a rocket sled, railgun, or other similar device. This stage would be optimized for heavy lift subsonic flight. After reaching a high enough cruise altitude, the primary vehicle (a hypersonic lifting body would be deployed). The second stage will use a standard turbine engine to accelerate to high enough speeds to operate a scramjet engine. Once the scramjet is operated and the vehicle reaches hypersonic speeds, the principle of waveriding (compression lift) will be utilized. A third stage will utilize traditional liquid rockets to provide thrust into space beyond the operating range of air breathing vehicles.

Chapter 3

Vehicle Sizing

FAHLLS consists of three stages. The first stage is a large subsonic carrier aircraft that will lift the second two stages up to an altitude of 50,000 feet before deployment. The second stage will be a combined cycle aircraft with a turbojet used for accelerating to supersonic speeds and a scramjet engine that will be activated once a high enough Mach number is reached. The second stage will accelerate to a high hypersonic speed and high altitude. The third stage is a liquid rocket that will be activated when the hypersonic vehicle has reached its maximum speed and altitude.

In sizing the stages, the calculations must be worked backwards from the third stage, as each stage is a payload of the previous stage. Launch to LEO requires a delta V of approximately 7780 m/s. Launching in an Eastward direction enables the required delta V to be reduced by utilizing the Earth's rotation. The delta V imparted by the Earth's rotation is reduced at high latitudes as compared to the Equator. All calculations were completed assuming a launch from 60 degrees north latitude, which is the assumed worst case scenario. At this latitude, the delta V that must be provided by the launch vehicle is 7548 m/s.

The third stage was sized utilizing the rocket equation:

$$MR = e^{\frac{dV}{I_{sp} * g_0}} \tag{3.1}$$

An I_{sp} of 400 sec was assumed for the third stage, which is typical for a LOX/LH2 propulsion system. The final velocity of the second stage and beginning velocity of the third stage was selected as Mach 15, which is 4754 m/s at 200,000 ft.

The second stage was sized in the same manner as the first stage with an I_{sp} of 2000 sec. The starting velocity of this stage is Mach 0.8 which is 236 m/s at 50,000 ft.

The calculations for the third and second stages provide the total mass of the payload of the first stage. Research on heavy lift aircraft has shown a typical percentage useful load in the 35-40% range. We assume a useful load as 60% of the gross mass. This higher value is assumed because the aircraft is unmanned. Therefore life support systems are not needed and the vehicle can be designed with a lower safety factor. Additionally, lighter materials are expected to be available.

For an initial estimate, payload fractions of 10% were selected for both the second and third stages. The results of these calculations can be seen below.

Table 3.1: 3rd Stage, 10% Payload Fraction

Starting Mach Number	15
Starting Velocity (m/s)	**4754.077198**
Ending Velocity (m/s)	7548
Propellant Isp (sec)	400
dV (m/s)	**2793.922802**
Mass Ratio	**2.038081388**
Payload Mass (kg)	100000
Payload Fraction (%)	10
Gross Mass (kg)	**1100000**
Burnout Mass (kg)	**539723.294**
Structure Mass (kg)	**439723.294**
Propellant Mass (kg)	**560276.706**
Structure Fraction	**0.439723294**
Propellant Fraction	**0.50934246**

Table 3.2: 2nd Stage, 10% Payload Fraction

Starting Mach Number	0.8
Starting Velocity (m/s)	**236.0066169**
Ending Velocity (m/s)	4754
Propellant Isp (sec)	2000
dV (m/s)	**4517.993383**
Mass Ratio	**1.258946037**
Payload Mass (kg)	1100000
Payload Fraction (%)	10
Gross Mass (kg)	**12100000**
Burnout Mass (kg)	**9611214.18**
Structure Mass (kg)	**8511214.18**
Propellant Mass (kg)	**2488785.82**
Structure Fraction	**0.773746744**
Propellant Fraction	**0.205684778**

Table 3.3: 1st Stage, 10% Payload Fraction

Payload Mass (kg)	12100000
Payload Fraction	0.6
GROSS TAKEOFF MASS (kg)	**20166666.67**

Payload fractions of each stage were then iterated on to find the optimal values. The results of this sizing analysis can be seen below.

Table 3.4: 3rd Stage, Optimal

Starting Mach Number	15
Starting Velocity (m/s)	**4754.077198**
Ending Velocity (m/s)	7548
Propellant Isp (sec)	400
dV (m/s)	**2793.922802**
Mass Ratio	**2.038081388**
Payload Mass (kg)	100000
Payload Fraction (%)	37.5
Gross Mass (kg)	**366666.6667**
Burnout Mass (kg)	**179907.7647**
Structure Mass (kg)	**79907.76466**
Propellant Mass (kg)	**186758.902**
Structure Fraction	**0.299654117**
Propellant Fraction	**0.50934246**

Table 3.5: 2nd Stage, Optimal

Starting Mach Number	0.8
Starting Velocity (m/s)	**236.0066169**
Ending Velocity (m/s)	4754
Propellant Isp (sec)	2000
dV (m/s)	**4517.993383**
Mass Ratio	**1.258946037**
Payload Mass (kg)	366666.6667
Payload Fraction (%)	35
Gross Mass (kg)	**1414285.714**
Burnout Mass (kg)	**1123388.67**
Structure Mass (kg)	**756722.0037**
Propellant Mass (kg)	**290897.0439**
Structure Fraction	**0.722325549**
Propellant Fraction	**0.205684778**

Table 3.6: 1st Stage, Optimal

Payload Mass (kg)	1414285.714
Payload Fraction	0.6
GROSS TAKEOFF MASS (kg)	**2357142.857**

The targeted case at 60 degrees latitude was used as the baseline. Current heavy lift aircraft may have wing loadings in the range of 600-850 kg/m^2. Assuming a wing loading of 680 kg/m^2, for the gross takeoff mass of 2,357,142.857 kg, the required wing area is approximately 3453.5 m^2 for the first stage. Multiple aspect ratios were considered and an aspect ratio of 8 was selected. This results in a wingspan of 166.22 m. While a larger aspect ratio would help prevent induced drag, it would also require a prohibitively large wingspan. An aspect ratio of 8 is a balance between low induced drag and an extremely large wingspan. The second and third stages are lifting bodies, and thus typical aircraft sizing calculations cannot be used.

The general shape for the second and third stages can be approximated by a delta-wing geometry. The aspect ratio was chosen to be 2, which is standard for a delta-wing geometry. For the second and third stages, wing area was selected based on lift considerations covered in subsequent sections of this report.

The gross mass of the second stage (including the third stage) is 1,414,285.71 kg; the gross weight for the third stage is 366,666.67 kg. The wing area is 15,541 m^2 for the second stage, and 458.33 m^2 for the third stage. For the second stage, the maximum wingspan is

thus 176.3 meters, while for the third stage, the maximum wingspan is 42.82 meters. The wing loading of the second stage is very low at 91 kg/m^2.

In order to calculate the takeoff speed of the first stage, airfoils that could be used were researched. It was found that the S1210 and Eppler 423 are ideal airfoils for a heavy lift aircraft. Each airfoil has a zero degree angle of attack lift coefficient of approximately 1.25. Using this lift coefficient it was found that the takeoff speed of the first stage would be 113.2 m/s at sea level. The landing mass of the first stage without the payload is 793,479.14 kg and the landing speed was calculated to be 71.58 m/s.

Delta-wings generally stall at higher angles of attack than rectangular wings; thus, at landing, the expected angle of attack is approximately 12 degrees. Using slender wing theory, the lift coefficient at landing is approximately 0.658. Assuming all fuel has been depleted (the second and third stages glide to a landing), the weights for the second and third stages at landing are 1,123,388.67 kg and 179,907 kg, respectively. At landing, the lift generated is approximately equal to weight. Thus, setting wing loading equal to dynamic pressure and solving for velocity, the landing velocities for the second and third stages are approximately 124.35 m/s and 97.73 m/s.

Chapter 4

Aerodynamics and Propulsion

4.1 Stage 1

As stated previously, an aspect ratio of 8 was chosen for the first stage. This was done as a balance between efficiency and structural concerns; too high of an aspect ratio might lead to structural failure, while a low aspect ratio is quite inefficient. The first stage flies to Mach 0.8, and an altitude of 50,000 feet. Using the standard atmosphere model, these conditions correspond to a dynamic pressure of 5291 Pascals.

Both parasite drag and induced drag were then calculated. The induced drag coefficient was calculated assuming a lift coefficient of 1.25 and Oswald efficiency factor of 0.9. The lift coefficient comes from the S1210 high lift airfoil. Induced drag was calculated as follows.

$$C_D = \frac{C_L^2}{\pi e A R} \tag{4.1}$$

Then, the actual drag force was calculated using the obtained value of dynamic pressure of 5291 Pa, and the previously estimated wing area of 3453.5 m2.

$$D_i = C_{D,i} \cdot q_\infty \cdot S = \frac{C_L^2}{\pi e A R} \cdot q_\infty \cdot S \tag{4.2}$$

The induced drag was found to be 1,262,000 Newtons, or 283,758 pounds.

Parasite drag was calculated using a $C_{D,0}$ of 0.02 which comes from drag plots for the S1210 airfoil. The parasite drag is calculated as follows.

$$D_0 = C_{D,0} \cdot q_\infty \cdot S \tag{4.3}$$

The worst-case was found to be 365,449 Newtons, or 82,156 pounds.

4.1.1 Skin Friction Drag

In addition to other forms of drag, skin friction drag due to viscous effects plays a role in the drag calculations. The method for calculating the skin friction drag is the same for all flight regimes, and is described below:

1. Find $\frac{T_0}{T}$ using $\frac{T_0}{T} = 1 + \frac{\gamma - 1}{2} M^2$.

2. Find T^* using $T^* = T_e(1 + 0.032M_e^2 + 0.58(\frac{T_w}{T_e} - 1))$.

3. Find ρ^* using $\rho^* = \frac{p}{RT^*}$.

4. Find μ^* using $\frac{\mu^*}{\mu} = (\frac{T^*}{T_0})^{\frac{3}{2}} \frac{T_0+110}{T^*+110}$.

5. Find Re_c^* using $Re_c^* = \frac{\rho^* U_\infty c}{\mu^*}$.

6. Skin Friction Drag

   (a) Turbulent Boundary Layer: Find C_f^* using $C_f^* = \frac{0.074}{(Re_c^*)^{1/5}}$

   (b) Laminar and Turbulent Boundary Layer: Find C_f^* using $C_f^* = \frac{1.328}{\sqrt{Re_T}} + \frac{0.074}{Re_c^{0.2}} - \frac{0.074}{Re_T^{0.2}}$ where Re_T is the transition Reynolds number.

7. Find D_f using $D_f = 2[\frac{1}{2}\rho^* U_e^2 S C_f^*]$

The transition from laminar to turbulent flow was assumed to occur at a local Reynolds number of 500,000. This corresponds to a worst case scenario of 0.78% chord and 2.11% chord for the first and second stages, respectively. For the first two stages, due to the negligible amount of the surface that has a laminar boundary layer, the entire boundary layer was modeled as turbulent. The boundary layer drag on the third stage includes both laminar and turbulent effects, as a significant portion of the wing's boundary layer is laminar.

For the first stage, an additional 67,500 N of drag was caused by skin friction. Thus, the total drag was estimated to be 1,694,941 Newtons.

The first stage carrier aircraft will use turbofan engines similar to what are used in large cargo and passenger aircraft currently. Our research has shown that the General Electric GE90 has a record thrust level of 130,000 lb. The rule of thumb for takeoff is that thrust should be 25-30% of GTOW. For our 2,357,142.86 kg first stage aircraft, 25% of the GTOW is 1,299,544.7 lb. Assuming future improvements allow thrust levels of 170,000 lb per engine, takeoff would require 8 engines operating at maximum thrust. Based on our cruise drag estimate, this drag could be overcome with 8 engines operating at 30% of maximum thrust during cruise. The required fuel load was calculated as 149,378 kg assuming a SFC of 0.3 lb/hr/lbf, a 2 hour flight time, and average thrust of 1.5x the cruise value (to account for takeoff and acceleration to cruise velocity). This fuel amount is 6.3% of our GTOW. Based on our setting that 60% of the GTOW is the payload, this leaves 33.7% of our GTOW as our structure.

4.2 Stage 2 and Stage 3

The second stage propels the vehicle from Mach 0.8 and 50,000 feet to Mach 15 and 200,000 feet. This poses difficulty in analysis, as this range of Mach numbers goes from subsonic to supersonic to hypersonic. The initial trajectory analysis attempts to simulate the flight of the second stage through the atmosphere. Mach number as a function of altitude was chosen to be parabolic in nature, biasing much of the acceleration of the vehicle in the upper altitudes of the flight envelope. This was done so as to increase the available lift of the vehicle

at higher altitudes due to rapidly decreasing freestream density, which in turn allows for a lower wing area and less mass. The Mach number as a function of altitude was represented by the following equation:

$$M = 6.3111 \times 10^{-10}(Alt - 50000)^2 + 0.8 \tag{4.4}$$

Because the vehicle's acceleration is biased towards the upper atmosphere in a parabolic fashion, so should the propellant consumption. Thus, the vehicle weight as a function of altitude should also follow a parabola. The vehicle mass versus altitude is represented by the following equation:

$$m = -1.2282 \times 10^{-5}(Alt - 50000)^2 + 1,414,286 \tag{4.5}$$

Vehicle weight at each altitude was found by multiplying the vehicle mass by gravitational acceleration at each altitude, which was found using Newton's law of gravitation. Atmospheric properties (pressure, density, temperature, speed of sound, and dynamic viscosity) used were taken from the 1976 standard atmosphere. 1000 simulation steps were used, equally spaced from 50,000 feet to 200,000 feet.

Plots of Mach number versus altitude and vehicle mass versus altitude are shown below in Figures 4.1 and 4.2, respectively.

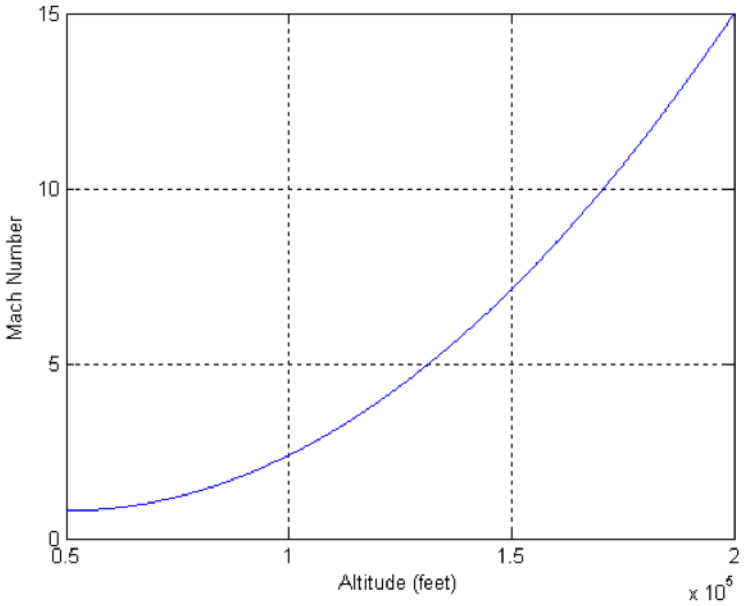

Figure 4.1: Stage 2 Mach number vs. altitude

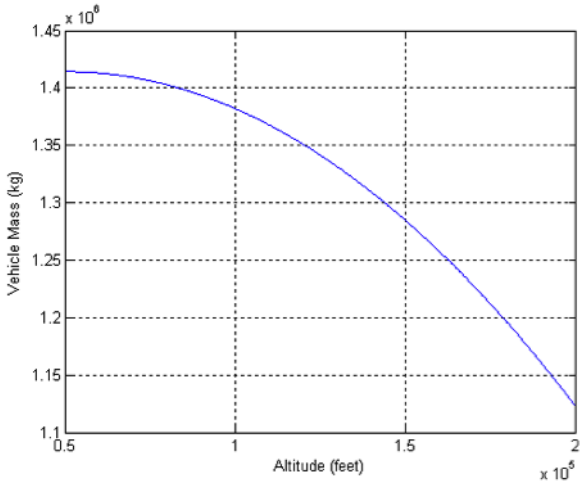

Figure 4.2: Stage 2 Mass vs. altitude

At each altitude, the corresponding Mach number was found. Lift at each point was calculated in order to determine the necessary angle of attack needed to fly at. The required angle of attack was defined as the angle of attack that would able to provide lift equal to 1.1 times the weight, in order to provide the vehicle the capability to accelerate upwards through the atmosphere. As previously stated, there are three main regimes in the flight of the second stage: subsonic, supersonic, and hypersonic. Each of these three regimes is now discussed.

4.2.1 Subsonic

Lift is given as follows:

$$L = 1.1 \times W = \frac{1}{2}\rho_\infty \, U_\infty^2 S C_L \tag{4.6}$$

Expressing velocity in terms of Mach number, and calculating lift coefficient using slender wing theory, the expression for lift can be rewritten as:

$$L = 1.1 \times W = \frac{1}{2}\rho_\infty M_\infty^2 \gamma R T_\infty S \frac{\pi}{2} AR\alpha \tag{4.7}$$

where α is in radians. Using the above equation given the vehicle weight and thus lift required, α can be solved for. For the subsonic regime, the required angles of attack were found to be very small, and the air was relatively dense, so thrust was not considered to significantly affect lift.

Then, given the required angle of attack, drag could be calculated. The induced drag from slender wing theory is given by:

$$C_{D,i} = \frac{C_L^2}{\pi AR} \tag{4.8}$$

4.2.2 Supersonic

For the supersonic regime, assumed to be from Mach 1 to Mach 4, two methods were used. As previously mentioned, the second stage is a delta-wing wedge, with a half angle of 10 degrees. At low Mach numbers, oblique shocks did not stay attached, and thus a bow shock was formed. Because the bow shock is entirely in front of the vehicle, the flow that the vehicle sees is subsonic, and slender wing theory was used, with the Mach number behind the shock (the Mach number that the vehicle sees) calculated using normal shock relations. When the Mach number was fast enough such that oblique shocks formed on the vehicle, shock-expansion theory was used to calculate the lift and drag. At each altitude, the lift at a wide range of angles of attack was calculated, using either slender wing theory (bow shock) or shock-expansion theory (oblique shocks). Then, linear interpolation was used to find the angle of attack required to equate lift to weight. Then, the drag at each altitude was calculated either via the same manner as shown previously for slender wing theory, or via shock-expansion theory. In addition, thrust times the sine of angle of attack was included in the lift calculations. Skin friction drag was also included and calculated as described in Section 4.1.1.

4.2.3 Hypersonic

For the hypersonic regime, assumed to be from Mach 4 to Mach 15, modified Newtonian hypersonic aerodynamics were used to calculate the lift (and thus required angle of attack) and drag. A similar solution method as used for the supersonic regime was used for the hypersonic regime. For a range of angles of attack, the lift and drag were calculated, and then linear interpolation was used to equate lift to weight (times the 1.1 load factor). Then, the drag corresponding to that angle of attack was also found via linear interpolation. Lift times the sine of angle of attack was also included in the lift calculations. Lift and drag calculation at each angle of attack are as follows.

First, the turn angles for the upper and lower surfaces were found using geometry:

$$\delta_u = \theta_u - \alpha \tag{4.9}$$

$$\delta_l = \theta_l + \alpha \tag{4.10}$$

Next, the maximum pressure coefficient was calculated:

$$c_{p,max} = \frac{\frac{p_{02}}{p_\infty} - 1}{\frac{\gamma}{2} M_\infty^2} \tag{4.11}$$

where

$$\frac{p_{02}}{p_\infty} = \left[\frac{(\gamma+1)^2 M_\infty^2}{4\gamma M_\infty^2 - 2(\gamma-1)}\right]^{\frac{\gamma}{\gamma-1}} \left[\frac{1-\gamma+2\gamma M_\infty^2}{\gamma+1}\right] \tag{4.12}$$

Next, pressure coefficient could be found on the upper and lower surfaces by

$$c_{p,l} = c_{p,max} \sin^2 \delta_l \tag{4.13}$$

$$c_{p,u} = c_{p,max} \sin^2 \delta_u \tag{4.14}$$

Then, C_N and C_C were calculated by

$$C_N = \frac{1}{c} \int_0^c (c_{p,l} - c_{p,u}) dx \tag{4.15}$$

$$C_C = c_{p,max} \sin^2 \delta_u \tan^2 \delta_u + c_{p,max} \sin^2 \delta_l \tan^2 \delta_l \tag{4.16}$$

Finally, lift and drag coefficients, and then lift and drag, were calculated:

$$C_L = C_N \cos \alpha - C_C \sin \alpha \tag{4.17}$$

$$C_D = C_N \sin \alpha + C_C \cos \alpha \tag{4.18}$$

$$L = \frac{1}{2} \rho_\infty \, U_\infty^2 S C_L + T \sin \alpha \tag{4.19}$$

$$D = \frac{1}{2} \rho_\infty \, U_\infty^2 S C_D \tag{4.20}$$

Skin friction drag was also included and calculated as described in Section 4.1.1

4.2.4 Stage 2 Simulation Results

MATLAB scripts used to complete the simulation can be found in the attachments included with this report. A plot of total drag versus altitude is shown below in Figure 4.3.

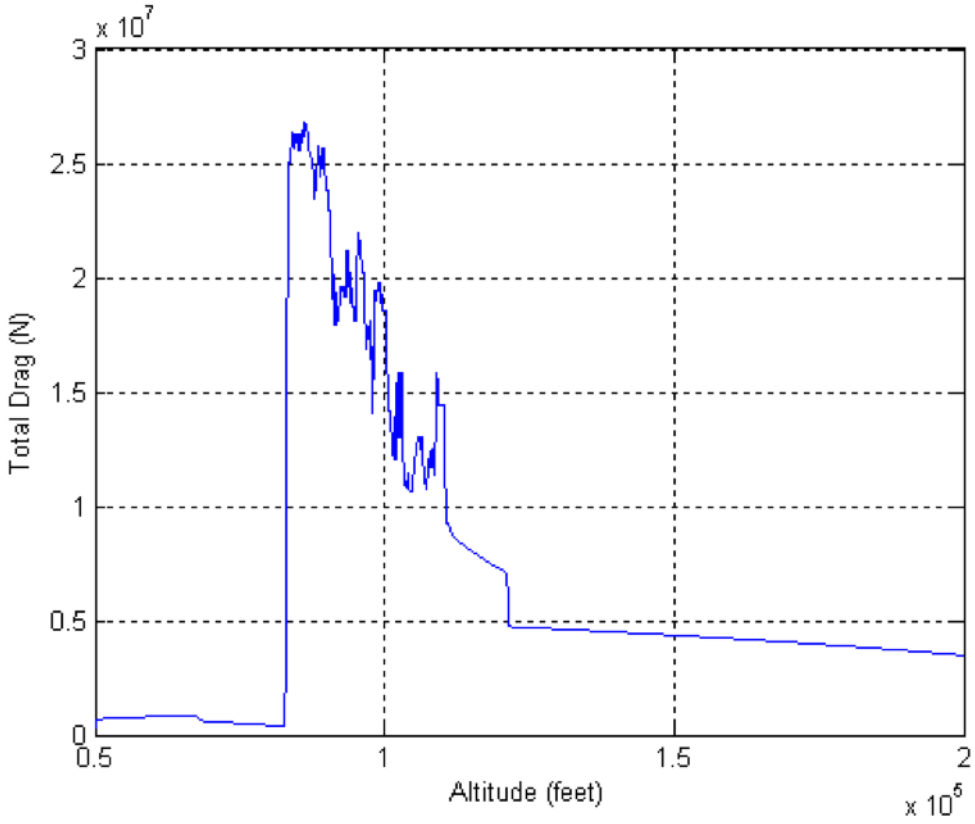

Figure 4.3: Stage 2 Total drag vs. altitude

The maximum drag is approximately 25 MN. The sudden rise in drag at approximately Mach 1.4 is when the shock waves first become attached to the vehicle, and thus represents the transition between slender wing theory and shock-expansion theory. In reality, the sudden rise might not be as much as it is in this first-order approximation, and it would likely be a more gradual transition. The drag is seen to be very erratic and non-continuous which is likely due to the interpolation method used in the calculations.

A plot of the pressure/induced drag vs. altitude can be seen in Figure 4.4.

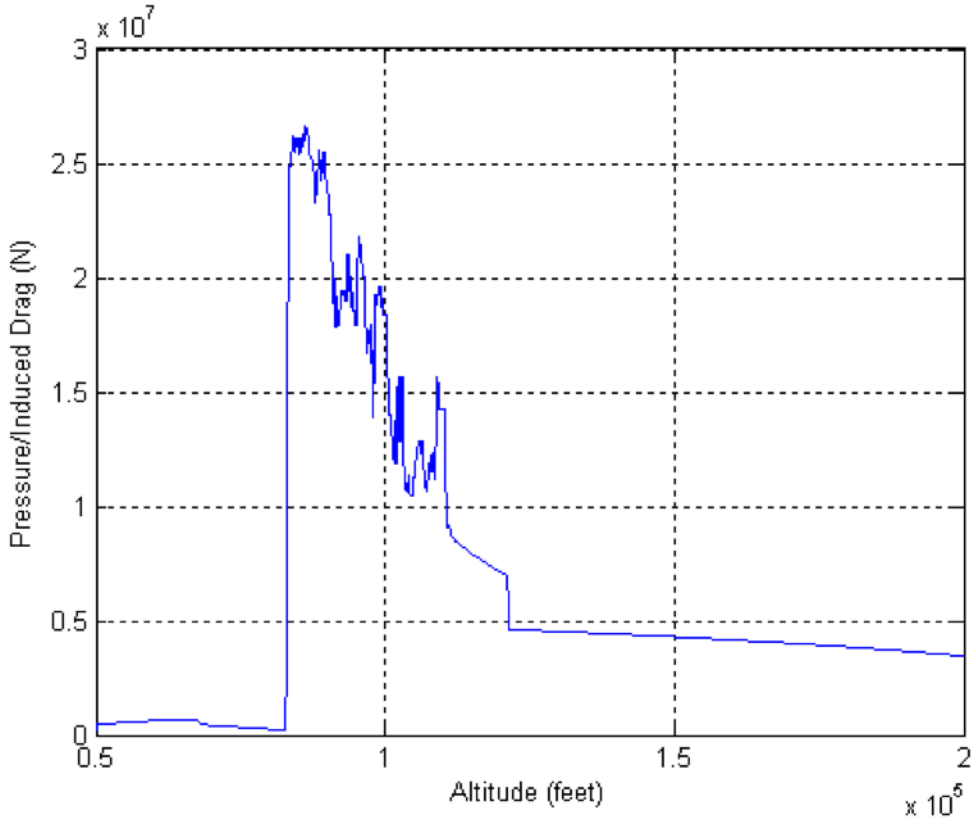

Figure 4.4: Stage 2 Induced/pressure drag vs. altitude

A plot of the pressure/induced drag vs. altitude can be seen in Figure 4.5.

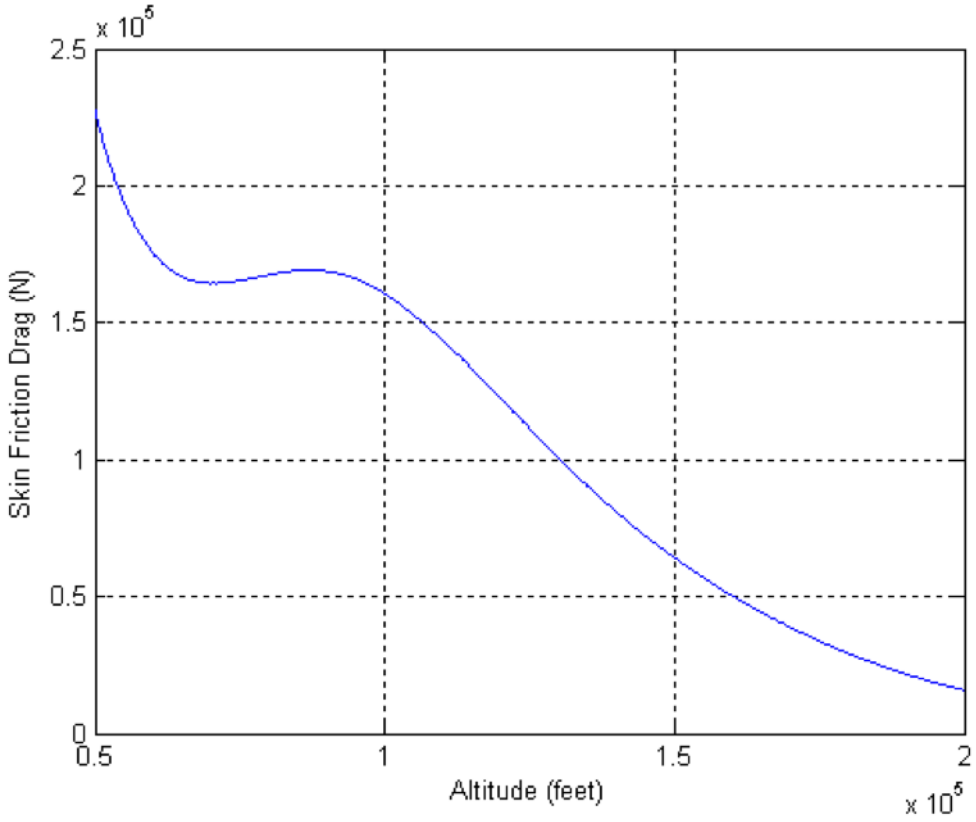

Figure 4.5: Stage 2 skin friction drag vs. altitude

A plot of the angle of attack vs. altitude can be seen in Figure 4.6.

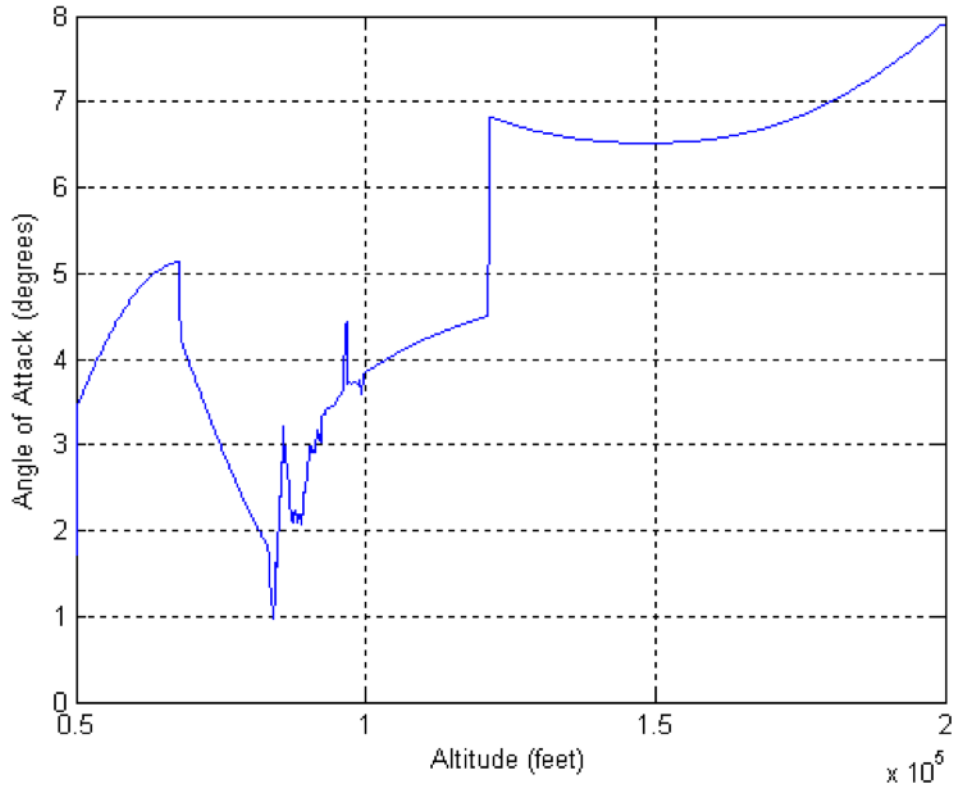

Figure 4.6: Stage 2 angle of attack vs. altitude

In order to accelerate the second stage from Mach 0.8 to Mach 15, a multimode engine will be required. NASA has performed tests for the Large-scale Inlet for Mode Transition Turbine-Based Combined-Cycle engine. This propulsion system would use a turbine engine for acceleration up to Mach 4. The variable geometry engine is then used to switch to a dual-mode ram/scramjet. NASA's current inlet was designed for flight at Mach 7. Scramjets are theoretically capable of flight at Mach 20+, so a modified version of NASA's LIMX TBCC should be capable of reaching Mach 15. Our sizing estimates were performed using the rocket equation modified to account for the high effective Isp of the ram/scramjet. These calculations take into account the 290,897.04 kg of fuel that must be carried. No thrust data is available for this theoretical design, but it is assumed that by the time this vehicle were developed the engine would be advanced enough to provide the necessary thrust of 35 MN.

4.2.5 Stage 3 Trajectory Simulation

The third stage starts at 200,000 feet and Mach 15, and accelerates the payload to 7780 m/s at 200 km (circular orbit velocity at this altitude). Due to the high freestream Mach numbers, modified Newtonian aerodynamics were used to calculate lift and drag. It is estimated that the third stage will reach approximately 280,000 feet (85.3 km) by the time it reaches Mach 20. Thus, the trajectory analysis of the third stage goes from Mach 15 and 200,000 feet to Mach 20 and 280,000 feet. The Mach number as a function of altitude was assumed to be a linear function; it is given by

$$M = 6.25 \times 10^{-5} \times Alt + 2.5 \tag{4.21}$$

At 280,000 feet, from the 1976 Standard Atmosphere model, the temperature is 186.95 K; thus, the speed of sound is 274.07 m/s. Thus, the velocity of the vehicle at this altitude is 5481 m/s. Thus, by the time the vehicle has reached this altitude, it has gone through a Δv of 727 m/s. According to the ideal rocket equation, the mass ratio required for this Δv is 1.2038. Thus, assuming a uniform propellant consumption, the vehicle mass at 280,000 feet is 304,599 kg, meaning that 62,068 kg of propellant has been burned. This is 33.23% of the propellant aboard the third stage. Vehicle mass as a function of altitude follows a linear function, given by

$$m = -0.77585 \times Alt + 521837 \tag{4.22}$$

Weight of the vehicle was again calculated by multiplying the mass by the gravitational acceleration at each altitude. 1000 simulation steps were used, equally spaced between 200,000 feet and 280,000 feet.

To calculate lift and drag, modified Newtonian Aerodynamics were used, as well as compressible boundary layer theory. The methodology to perform these calculations are identical to that used in the stage 2 trajectory simulation.

Plots of Mach number versus altitude and vehicle mass versus altitude are shown below in Figures 4.7 and 4.8.

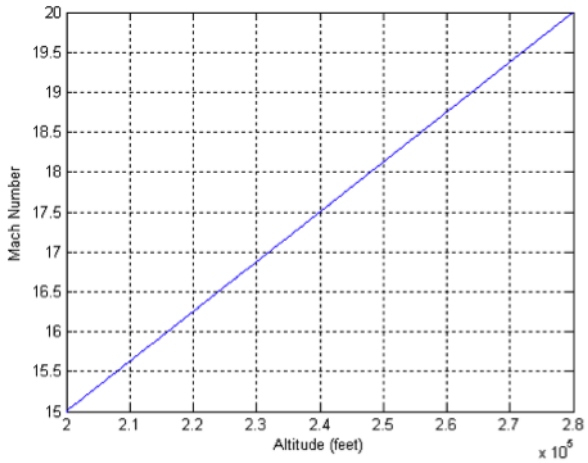

Figure 4.7: Stage 3 Mach number vs. altitude

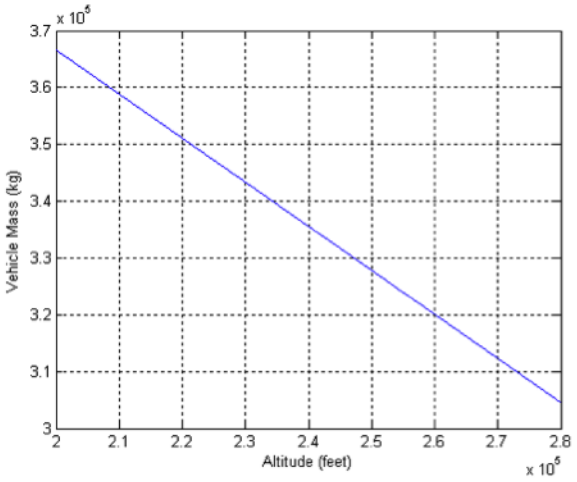

Figure 4.8: Stage 3 mass vs. altitude

4.2.6 Stage 3 Trajectory Simulation Results

The results for stage 3 are much smoother, with no discontinuities, than the stage two simulation, because only one aerodynamic theory was used. Due to the drastically decreased density, drag is much lower for the third stage than the second stage. As a result of the much lower freestream density, the third stage generally needs to maintain a larger angle of attack than the second stage.

A plot of total drag versus altitude is shown below in Figure 4.9.

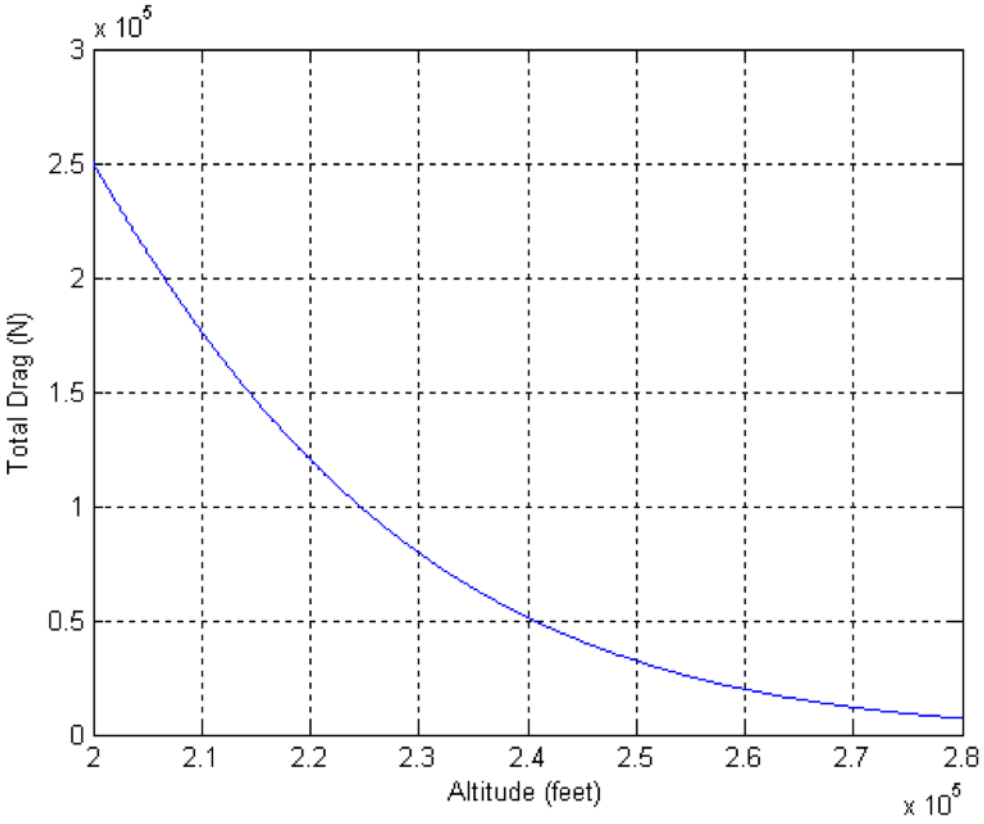

Figure 4.9: Stage 3 Total drag vs. altitude

A plot of the pressure/induced drag vs. altitude can be seen in Figure 4.10.

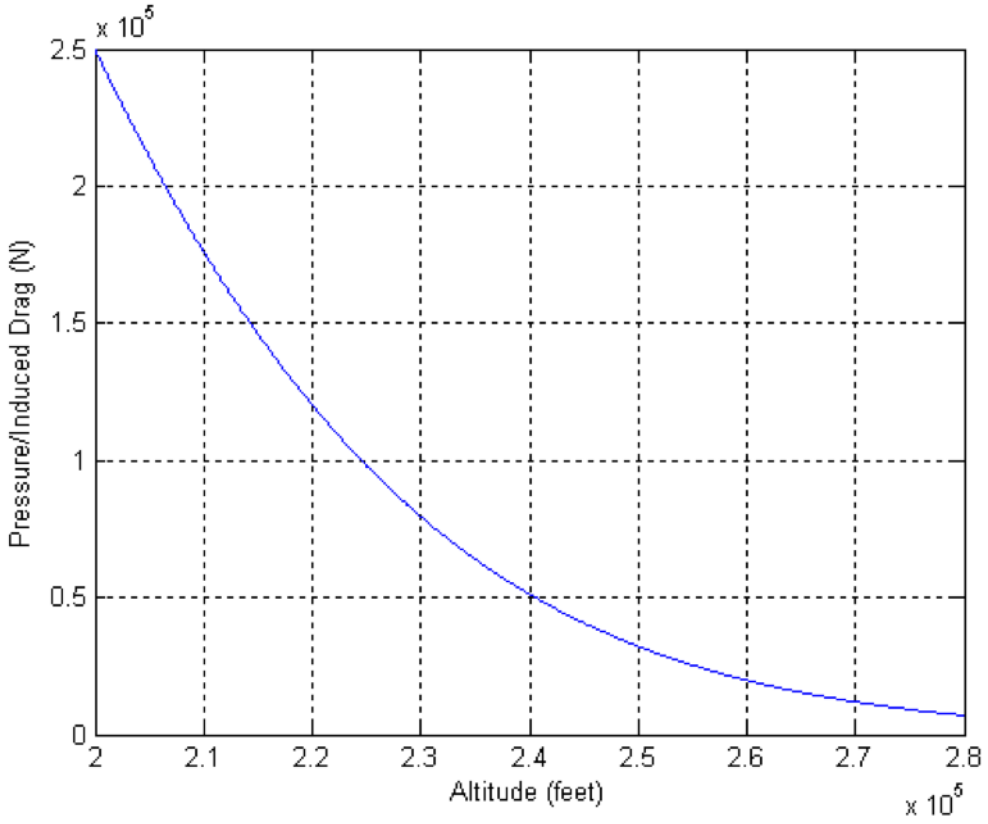

Figure 4.10: Stage 3 Induced/pressure drag vs. altitude

A plot of the pressure/induced drag vs. altitude can be seen in Figure 4.11.

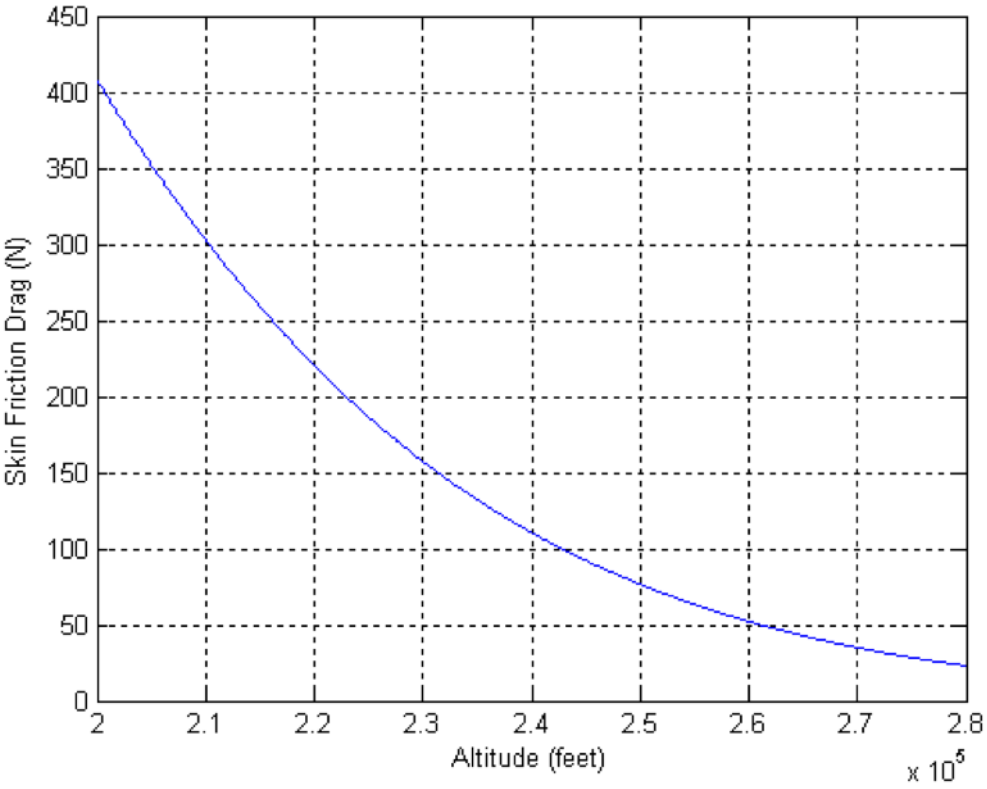

Figure 4.11: Stage 3 skin friction drag vs. altitude

A plot of the angle of attack vs. altitude can be seen in Figure 4.12.

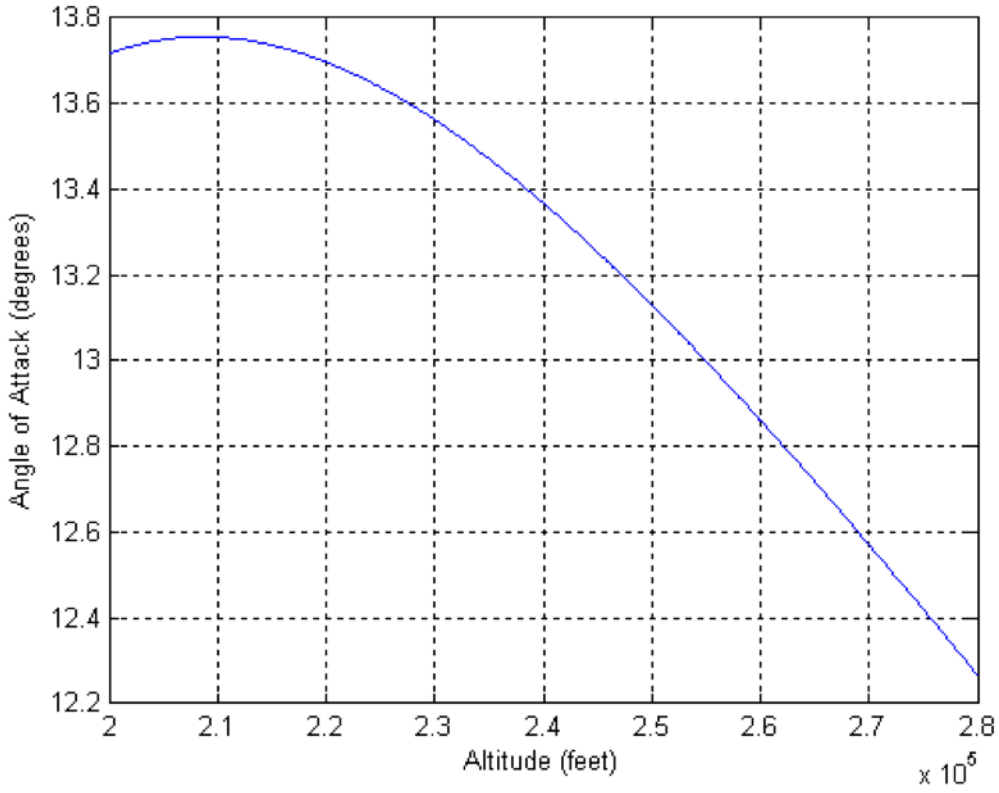

Figure 4.12: Stage 3 angle of attack vs. altitude

The sizing of third stage was completed assuming an LH2/LOX liquid rocket engine would be used. The sizing was completed using the rocket equation and takes into account the 186,758.9 kg of fuel which must be carried on the vehicle. The maximum estimated drag of 250,000 N can easily be overcome by current propulsion technology. This is approximately 11% of the maximum thrust of a Space Shuttle Main Engine (the most efficient LH2/LOX designed to date).

Chapter 5

Conclusion

FAHLLS was intended to be a reusable launch system with a rapid turnaround time, in order to make frequent deliveries to low Earth orbit. All stages are designed to be reusable, drastically decreasing the cost of the launch system. FAHLLS is physically quite large in size and requires large amounts of thrust. Despite the large size, our work has shown that the first and third stages are somewhat feasible with current propulsion technology. The first stage will require improvements of thrust capability in turbofan engines, or it will require more engines. The second stage requires advancement in ramjet and scramjet technology, but may be achievable in the next 25-50 years as these technologies advance. Advances in materials and construction technology are also necessary to bring this system within reach. FAHLLS as designed is intended to be able to achieve the goals of Space Solar Power and eliminate the need for use of fossil fuels on Earth within the next 50 years.

Bibliography

[1] J.D. Saunders et. al. NASA Glenn Research Center. *Inlet Mode Transition Screening Test for a Turbine-Based Combined-Cycle Propulsion System.* May 13, 2008. *https : //rt.grc.nasa.gov/files/*2008 − *center* − *best* − *paper* − *saunders* − *etal* − *jun*2009.*pdf*

[2] Philip T. Harsha et. al. ATK. *X-43A Vehicle Design and Manufacture. http : //pdf.aiaa.org/preview/CDReadyMISPHST*$05_1$136/*PV*$2005_3$334.*pdf*

[3] *Faster Than a Speeding Bullet: Guinness Recognizes NASA Scramjet.* June 20, 2005. *http : //www.nasa.gov/home/hqnews/*2005/*jun*/$HQ_05_156_X43A_G$*uinness.html*

[4] Astronomy Picture of the Day. *NASA's X-43A Scramjet Sets Air Speed Record* March 29, 2004. *http : //apod.nasa.gov/apod/ap*040329.*html*

[5] *X-51A Waverider.* March 23, 2011. *http : //www.af.mil/information/factsheets/factsheet.asp?fsI1*

[6] *X-51 Waverider makes historic hypersonic flight.* May 26, 2010. *http : //www.af.mil/news/story.asp?id* = 123206525

[7] *X-51.* May 20, 2010. *http : //www.af.mil/shared/media/photodb/photos/*100520 − *F* − 9999*B* − 111.

[8] Stephen Trimble. *DARPA cancels Blackswift hypersonic test bed.* October 13, 2008. *http : //www.flightglobal.com/news/articles/videos* − *darpa* − *cancels* − *blackswift* − *hypersonic* −

[9] *Falcon HTV-3X. http : //www.youtube.com/watch?v* = 8*MhtLWB*0*dJ*8

[10] Encyclopedia Astronautica. *X-30. http : //www.astronautix.com/lvs/x*30.*htm*

[11] XCOR Aerospace *XR-5K18, LOX / Kerosene "Lynx" engine. http : //xcor.com/products/engines/*$5K18_LOX - kerosene_rocket_e$*ngine.html*

[12] XCOR Aerospace *Lynx Development Plan. http : //xcor.com/products/vehicles/lynx*$_d$*evelopment.htr*

[13] XCOR Aerospace *About Lynx. http : //xcor.com/products/vehicles/lynx*$_s$*uborbital.html*

[14] David Darling. *HOTOL. http : //www.daviddarling.info/encyclopedia/H/HOTOL.html*

[15] *HOTOL. http : //upload.wikimedia.org/wikipedia/commons/d/d*1/*HOTOL.JPG*

[16] *HOTOL. https : //www.princeton.edu/ achaney/tmve/wiki*100*k/docs/HOTOL.html*

[17] Encyclopedia Astronautica. *HOTOL. http : //www.astronautix.com/lvs/hotol.htm*